Angewandte Chemie
Eine Zeitschrift der Gesellschaft Deutscher Chemiker

Supporting Information

69451 Weinheim, Germany

Photoinduced Gold(I)–Gold(I) Chemical Bonding in Dicyanoaurate Oligomers**

Ganglong Cui, Xiao-Yan Cao, Wei-Hai Fang, Michael Dolg,* and Walter Thiel**

anie_201305487_sm_miscellaneous_information.pdf

Table of Contents

1 Computational Methods

Stationary points on the S_0 potential energy surface in aqueous solution were optimized using Møller-Plesset second-order perturbation theory (MP2). [1] This method has been demonstrated to be sufficiently accurate for modeling the non-covalent aurophilic interaction, [2, 3] which is responsible for the formation of oligomers in the S_0 state. By contrast, excited-state gold oligomers contain predominantly covalent Au-Au metal bonds. Density functional theory (DFT) does not treat the aurophilic interaction well, [4] but should be suitable for describing covalent bonding in the excited states. Hence, we employed conventional DFT [5] and linear-response time-dependent DFT (TD-DFT) [6] with the range-separated CAM-B3LYP exchange-correlation functional [7–10] to optimize the stationary points on the T_1 and S_1 excited-state energy surfaces. In all optimizations, the polarizable continuum model (PCM) [11, 12] was adopted to implicitly account for solvent effects. Scalar relativistic effects were included for Au by means of the Cowan-Griffin-adjusted shape-consistent small-core pseudopotential (PP) of Hay and Wadt [13], and the corresponding improved valence basis set LANLTZf [14] was applied. C and N were treated at the (non-relativistic) all-electron level using the 6-31G* basis set [15]. This combination of Au PP and basis sets has previously been shown to perform well for dicyanoaurate oligomers $[Au(CN)_2^-]_n$. [16]

Multi-state (MS) complete-active-space second-order perturbation theory (CASPT2) [17] was employed to refine the single-point energies for all optimized structures. In the MS-CASPT2 calculations, three [two] roots with equal weights were used for singlets [triplets]. The Cholesky decomposition [18] and the imaginary shift technique (0.3 a.u.) [19] were applied. To account for solvent effects, the conductor-like version of the polarizable continuum model (PCM) [11, 12] was also used in the MS-CASPT2 calculations, with an average area for the surface elements of the cavity boundary of 0.2 Å^2 for the dimer and 0.4 Å^2 for the other oligomers. Au was described by the relativistic small-core PP of Hay and Wadt together with the original LANL2DZ valence basis set. [13] C and N were again treated at the all-electron level using the 6-31G* basis set [15].

To validate the DFT(CAM-B3LYP) and TDDFT(CAM-B3LYP) performance, we performed *ab initio* geometry optimizations of the dimer structures using the resolution-of-identity second-order approximate coupled-cluster approach (RI-CC2), algebraic diagrammatic construction (RI-ADC(2)), and Møller-Plesset method (RI-MP2) [20–25]. In this validation work, the error-balanced def2-SVP and def2-TZVP basis sets of Weigend and Ahlrichs were used for all atoms, [26] and scalar-relativistic effects were included for the Au atom by means of the Wood-Boring-adjusted small-core PP of Andrae et al. [27] Solvent effects were not taken into account, since the TURBOMOLE software only allows the combination of RI-CC2 with the conductor-like screening model (COSMO) [28]; this is adequate for ground states but not for excited states, which require a state-specific PCM treatment. Thus, we performed the calibration against *ab initio* reference data *in vacuo*.

Born-Oppenheimer molecular dynamics (BOMD) simulations were run to estimate the bent-to-linear relaxation time of the staggered trimer in aqueous solution (PCM model). The equation of motions were integrated

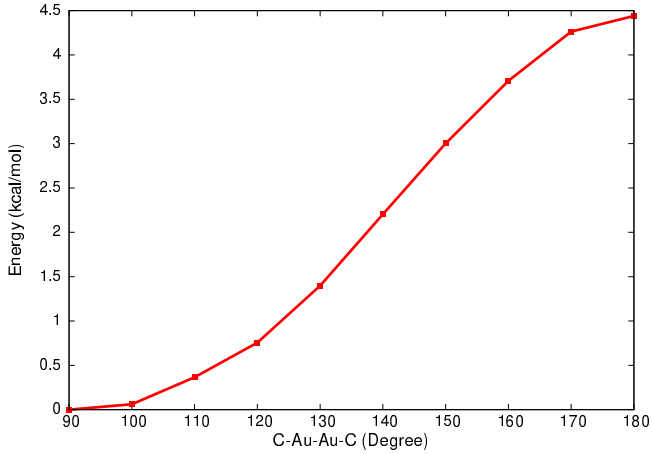

Figure 1: The ground-state MP2/PCM potential energy profile of the dicyanoaurate dimer with respect to the C-Au-Au-C dihedral angle.

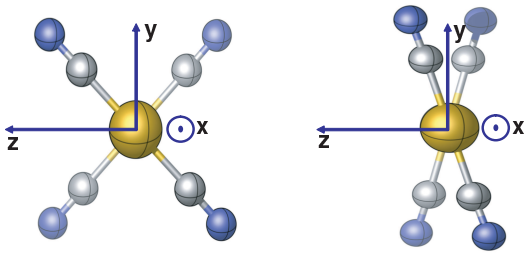

Figure 2: Staggered (left) and eclipsed (right) conformation of the dimer. The second Au atom lies behind the first one and is thus invisible. The x axis is along the Au-Au bond (perpendicular to the paper plane).

using a stepsize of 1.000 sqrt(amu)*bohr, the Bulirsch-Stoer method, and a fifth-order polynomial fitting correction scheme. The translational and rotational motions were projected out in each propagation step.

All MP2, DFT(CAM-B3LYP), and TD-DFT(CAM-B3LYP) calculations employed the GAUSSIAN09 package; [29] all MS-CASPT2 calculations were performed with the MOLCAS7.6 package; [30, 31] all RI-CC2, RI-ADC(2), and RI-MP2 calculations were done with the TURBOMOLE6.3 package. [32]

2 Eclipsed-Staggered Potential Energy Profile in the S_0 State

The eclipsed conformation of the $[Au(CN)_2^-]_2$ dimer is not a minimum in the S_0 state, but lies only ca. 4 kcal/mol higher than the staggered conformation at the MP2/PCM level (see Fig. 1). Thus, in rigid surroundings such as in crystals and certain aggregates, the eclipsed structure may become a minimum. [33] The two conformers are depicted in Fig. 2.

3 DFT and TDDFT Performance

DFT was not used for ground-state optimizations because of its inadequate description of the non-covalent Au-Au aurophilic interaction. [4] DFT(CAM-B3LYP) and TD-DFT(CAM-B3LYP) were applied for the calculation of the T_1 and S_1 excited states, where the Au-Au metal bonding is predominantly covalent. These DFT methods can be combined with the state-specific PCM model to treat solvent effects in an implicit manner.

Table 1 lists the Au-Au bond lengths in the staggered conformation of the S_0, T_1, and S_1 states of $[Au(CN)_2^-]_2$, as calculated here and in previous work. The first-principles approaches (DFT, CC2 and MP2) give an Au-Au bond length between 2.96 and 3.17 Å for the S_0 ground state in vacuo, whereas an early extended Hückel calculation [3] reported a somewhat shorter distance of 2.88 Å. In the T_1 state, all methods predict a significant shortening of the Au-Au bond length compared with the S_0 state (by 0.3–0.6 Å, e.g. RI-CC2/def2-TZVP by 0.47 Å and CAM-B3LYP by 0.46 Å); the computed Au-Au bond length from CAM-B3LYP (2.71 Å) is slightly larger than the values obtained from RI-ADC(2), RI-CC2, and MP2 (2.58–2.66 Å). The results for the S_1 state are similar to those for the T_1 state.

In the ground state, the dicyanoaurate dimer is held together by the rather weak noncovalent aurophilic interaction (ca. 0.1 eV), which is comparable in strength to other weak noncovalent interactions, such as the dispersion interaction between neighboring cyano groups and the interactions with the solvent. Accordingly, the optimized Au...Au distance of the staggered dimer in the S_0 state is sensitive to the chosen *ab initio* electronic structure method (see Table 1) and to solvent effects (decrease of the MP2 value by 0.16 Å when going from the gas phase to aqueous solution). By contrast, the predominantly covalent Au-Au bond in the excited states is less sensitive (see e.g. the almost identical CAM-B3LYP distance in the gas phase and in aqueous solution). Comparison of the results for different basis sets shows that our chosen LANL2TZf ECP basis set gives Au-Au bond lengths that are very close to those obtained with larger basis sets (see Table 2).

In summary, the chosen methods (MP2/PCM for S_0, CAM-B3LYP/PCM for T_1, and TD-CAM-B3LYP/PCM for S_1) are found to be reasonably accurate overall, and thus suitable to describe the structures of dicyanoaurate oligomers in the ground and excited states.

4 Spectroscopic Data

To clarify the spectral assignments, we calculated at the MS-CASPT2/PCM and TD-CAM-B3LYP/PCM level the transition energies for the absorption, fluorescence, and phosphorescence spectra of $[Au(CN)_2^-]_n$ ($n = 2 - 5$). Table 3 collects the relevant results.

The absorption spectrum of dicyanoaurate in solution exhibits an increasing red shift with increasing solute concentration. [2] In dilute solution (i.e. 1.0×10^{-2} M), the absorption spectrum shows a low-energy band in the

Table 1: Au-Au Bond Lengths (Å) in the Staggered Conformation of the S_0, T_1, and S_1 States of $[Au(CN)_2^-]_2$ Calculated by Various Methods

State	This Work[a] (in water)	This Work[b] (in vacuo)	RI-ADC(2)[c1] (in vacuo)	RI-CC2[c1] (in vacuo)	RI-CC2[c2] (in vacuo)	MP2[d] (in vacuo)	EHT[d] (in vacuo)
S_0	3.01	3.17	3.17[e]	3.05	3.15	2.96	2.88
T_1	2.70	2.71	2.60	2.58	2.64	2.66	2.47
S_1	2.72		2.62	2.61	2.67		

[a]MP2/PCM for S_0, CAM-B3LYP/PCM for T_1, and TD-CAM-B3LYP/PCM for S_1; Au: LANL2TZf; C, N: 6-31G*.
[b]MP2 for S_0, and CAM-B3LYP for T_1; Au: LANL2TZf; C, N: 6-31G*.
[c1]Au: ECP60MWB, def2-TZVP; C, N: def2-TZVP.
[c2]Au: ECP60MWB, def2-SVP; C, N: def2-SVP.
[d]MP2 and Extended-Hückel theory (EHT) results of Rawashdeh-Omary et al. [3]
[e]RI-MP2 calculations using TURBOMOLE6.4.

Table 2: Au-Au Bond Lengths (Å) of the $[Au(CN)_2^-]_2$ Dimer in the Staggered Conformation of the S_0 Ground State Calculated with Different Basis Sets at the MP2/PCM(aqueous)/MP2(vacuo) Level

State	[a]cc-pVDZ	[a]cc-pVTZ	[b]def2-TZVP	[c]6-31G*	[d]6-31G*
S_0	3.01/3.15	2.95/3.12	2.98/3.15	3.20/	3.01/3.17
T_1	2.70/2.72	2.69/2.71	2.70/2.71		2.70/2.71

[a]MCDHF/DC+B-adjusted small-core PP and cc-pVDZ-PP basis set for Au [34, 35]
[b]WB-adjusted small-core PP and def2-TZVPPD basis set for Au [27, 36]
[c]CG-adjusted small-core PP and LANL2DZ basis set for Au [13]
[d]CG-adjusted small-core PP and LANL2TZf for Au [14]

250-270 nm region. On the basis of our computations, this band corresponds to the bright $S_0 \rightarrow S_1$ electronic excitation (245 nm) of the staggered dimer structure; however, a contribution from the staggered bent trimer structure (256 nm) cannot be completely excluded. When the solute concentration is increased to 0.3 M, an absorption band around 310 nm appears, which has commonly been ascribed exclusively to the trimer. [2, 16] Our theoretical work supports this experimental viewpoint but provides further insight: this band does not arise from the $S_0 \rightarrow S_1$ electronic transition in the staggered bent trimer (256 nm), but from the staggered linear trimer (293 nm); and the staggered linear tetramer (313 nm) could also provide a minor contribution. The estimated absorption maximum (326 nm) of the staggered linear pentamer matches with the experimental absorption band (330-350 nm) that appears at solute concentrations of 0.50-0.76 M. [2]

The emission spectra are more complicated because of the mixing of fluorescence and phosphorescence. Patterson et al. observed 5 emission bands (**I**, **II**, **III**, **IV**, and **V**) by varying the concentration, excitation wavelength, solvent, and temperature (see Figure 9 and Table 4 in their work [3]). Band **I** at 275-285 nm was assumed to come from dimer emission, but the character of the emitting state remained unclear. Our results indicate that this band should correspond to fluorescence from both dimer species (staggered at 274 nm and eclipsed at 289 nm). The experimental measurement for this emission was monitored using the 250 nm excitation wavelength, which concides with the absorption maximum computed for the staggered dimer structure (250 nm, see Table 3). Band **II** at 320-350 nm was assigned only to the trimer; [3] according to our calculations, both fluorescence

Table 3: MS-CASPT2/PCM and TD-CAM-B3LYP/PCM Vertical Transition Energies/Wavelengths (units: eV/nm) of Dicyanoaurate Oligomers in Aqueous Solution[a]

oligomers	absorption		fluorescence		phosphorescence	
$[Au(CN)_2^-]_2$	staggered		staggered	eclipsed	staggered	eclipsed
	4.96/250		4.52/274	4.30/289	3.83/323	3.83/324
	5.07/245		4.74/262	4.38/283	3.84/323	3.92/316
[b]$[Au(CN)_2^-]_3$	bent	linear		linear		linear
	4.84/256	4.23/293		3.77/329		3.26/381
	4.61/269	4.37/284		4.06/306		3.27/380
[c]$[Au(CN)_2^-]_4$		3.97/313		3.67/330		2.88/430
		3.96/313		3.73/332		3.03/409
[c]$[Au(CN)_2^-]_5$		3.80/326		3.42/362		2.76/449
		3.72/334		3.53/351		2.92/425

[a]MS-CASPT2 values in the first line and TD-CAM-B3LYP/PCM values in the second line; [b]staggered conformation; [c]staggered linear structure.

from the staggered linear trimer (329 nm) and phosphorescence from both dimer species (staggered at 323 nm and eclipsed at 324 nm), as well as fluorescence from the staggered linear trimer (330 nm), can contribute to this band **II**. The interpretation of band **III** at 380-390 nm is straightforward as it relates only to phosphorescence emission from the trimer. Band **IV** at 420-440 nm may be ascribed to phosphorescence from the staggered linear tetramer (430 nm), while band **V** at 455-470 nm possibly correlates with phosphorescence from the staggered linear pentamer (449 nm).

5 Excimer and Exciplex Analysis

The term *excimer* was introduced by Stevens and Hutton [37] in the 1960s and was later redefined by Birks as "a dimer which is associated in an excited electronic state and which is dissociative (i.e. would dissociate in the absence of external restraints) in its ground electronic state." [38, 39] Excimer formation is governed by the configurational mixing of diabatic exciton ($A^*A \leftrightarrow AA^*$) and charge resonance states ($A^+A^- \leftrightarrow A^-A^+$). In the case of weak coupling, the electronic excitation is localized on one of the two monomers and in this instance, the diabatic electronic wavefunction is almost identical to the adiabatic one; in the case of strong coupling, the electronic excitation is delocalized over both monomers and the adiabatic electronic wavefunction is represented as a linear combination of the above diabatic resonance states. [40, 41] Based on these general rules, we have analyzed the dicyanoaurate excimers and exciplexes optimized in this work.

The dimer of $[Au(CN)_2^-]_2$ belongs to the case of strong coupling because both HOMO and LUMO are delocalized fully over the two monomers (see the middle panel of Figure 2 in the main paper), and only one S_1 or T_1 minimum with pronounced Au-Au bond shortening (ca. 2.7 Å) is obtained in optimizations without any geometric constraints. [40]

In the trimer, the two Au-Au bond lengths are almost evenly shortened to ca. 2.8 Å in the T_1 and S_1 states

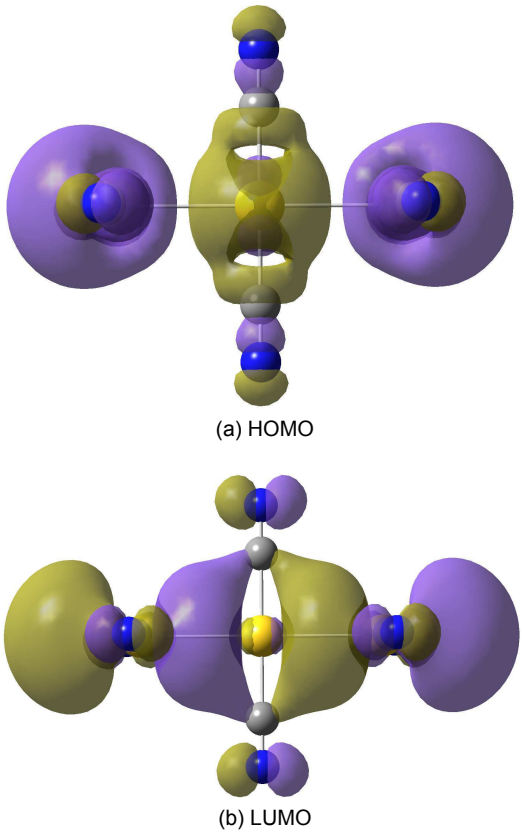

Figure 3: TD-CAM-B3LYP/PCM computed HOMO (a) and LUMO (b) (isosurface: 0.02) of the staggered linear trimer at the S_1 minimum.

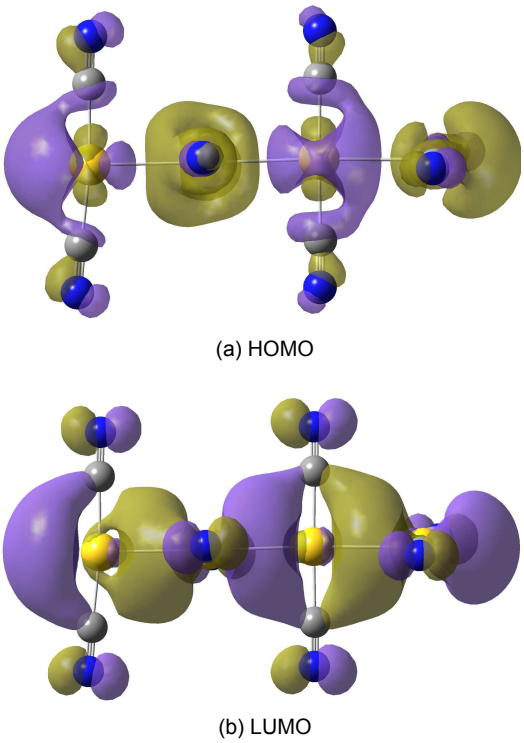

Figure 4: TD-CAM-B3LYP/PCM computed HOMO (a) and LUMO (b) (isosurface: 0.02) of the staggered linear tetramer at the S_1 minimum.

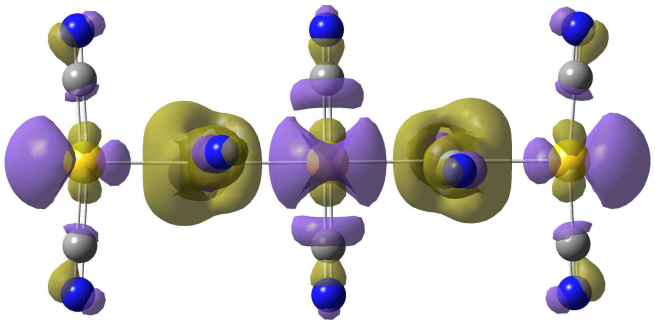

(a) HOMO

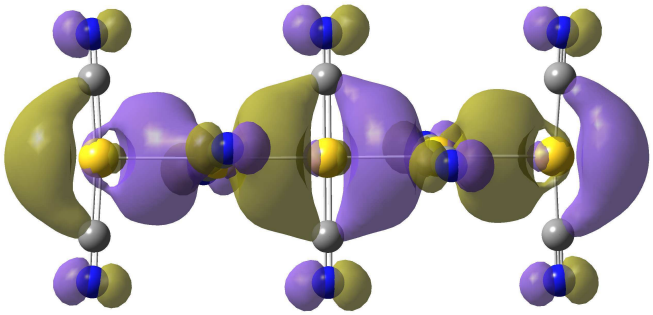

(b) LUMO

Figure 5: TD-CAM-B3LYP/PCM computed HOMO (a) and LUMO (b) (isosurface: 0.02) of the staggered linear pentamer at the S_1 minimum.

(see Figure 1 in the main paper). Analysis of the relevant orbitals (see Fig. 3) supports exciplex formation with strong coupling.

In the tetramer and pentamer, however, the middle Au-Au bonds become significantly shorter than those on the two sides. More interestingly, the terminal Au-Au bonds in the staggered pentamer are of similar length in the S_0, T_1, and S_1 states, and it is only the middle two bonds that are shortened in the excited states. Therefore, in comparison with the trimer, the tetramer and pentamer look more "like" an exciplex with some ground-state features, since the excited-state Au-Au bond shortening is spatially local. In the excited states of the dicyanoaurate oligomers, the strong coupling regime thus does not extend beyond two neighboring Au-Au bonds. Fig. 4 and Fig. 5 show the relevant orbitals of the tetramer and the pentamer, respectively.

References

[1] C. Møller, M. Plesset, Note on an approximation treatment for many-electron systems, Phys. Rev. 46 (1934) 618.

[2] M. Rawashdeh-Omary, M. Omary, H. Patterson, Oligomerization of Au(CN)2- and Ag(CN)2- ions in solution via ground-state aurophilic and argentophilic bonding, J. Am. Chem. Soc. 122 (2000) 10371.

[3] M. Rawashdeh-Omary, M. Omary, H. Patterson, J. Fackler Jr, Excited-state interactions for oligomers in solution. Formation of luminescent gold-gold bonded excimers and exciplexes, J. Am. Chem. Soc. 123 (2001) 11237.

[4] S. Wang, W. Schwarz, Quasi-relativistic density functional study of aurophilic interactions, J. Am. Chem. Soc. 126 (2004) 1266.

[5] R. G. Parr, W. T. Yang, Density-Functional Theory of Atoms and Molecules, Oxford University Press, USA, 1994.

[6] M. A. L. Marques, C. A. Ullrich, F. Nogueira, A. Rubio, K. Burke, E. K. U. Gross, Time-dependent Density Functional Theory, Springer, 2006.

[7] T. Yanai, D. P. Tew, N. Handy, A new hybrid exchange-correlation functional using the Coulomb-attenuated method CAM-B3LYP, Chem. Phys. Lett. 393 (2004) 51.

[8] C. Lee, W. Yang, R. Parr, Development of the Colle-Salvetti correlation-energy formula into a functional of the electron density, Phys. Rev. B 37 (1988) 785.

[9] A. Becke, Density-functional exchange-energy approximation with correct asymptotic behavior, Phys. Rev. A 38 (1988) 3098.

[10] A. D. Becke, A new mixing of Hartree-Fock and local density-functional theories, J. Chem. Phys. 98 (1993) 1372.

[11] V. Barone, M. Cossi, Quantum calculation of molecular energies and energy gradients in solution by a conductor solvent model, J. Phys. Chem. A 102 (1998) 1995.

[12] R. Improta, V. Barone, G. Scalmani, M. Frisch, A state-specific polarizable continuum model time-dependent density functional theory method for excited-state calculations in solution, J. Chem. Phys. 125 (2006) 054103.

[13] P. Hay, W. Wadt, Ab initio effective core potentials for molecular calculations. Potentials for K to Au including the outermost core orbitals, J. Chem. Phys. 82 (1985) 299.

[14] L. Roy, P. Hay, R. Martin, Revised basis sets for the LANL effective core potentials, J. Chem. Theory Comput. 4 (2008) 1029.

[15] R. Ditchfield, W. J. Hehre, J. A. Pople, Self-consistent molecular orbital methods. 9. Extended Gaussian-type basis for molecular-orbital studies of organic molecules, J. Chem. Phys. 54 (1971) 724.

[16] M. Iwamura, K. Nozaki, S. Takeuchi, T. Tahara, Real-time observation of tight Au-Au bond formation and relevant coherent motion upon photoexcitation of oligomers, J. Am. Chem. Soc. 135 (2012) 538.

[17] K. Andersson, P. Malmqvist, B. Roos, Second-order perturbation theory with a complete active space self-consistent field reference function, J. Chem. Phys. 96 (1992) 1218.

[18] J. Boström, M. Delcey, F. Aquilante, L. Serrano-Andrés, T. Pedersen, R. Lindh, Calibration of Cholesky auxiliary basis sets for multiconfigurational perturbation theory calculations of excitation energies, J. Chem. Theory Comput. 6 (2010) 747.

[19] N. Försberg, P. Malmqvist, Multiconfiguration perturbation theory with imaginary level shift, Chem. Phys. Lett. 274 (1997) 196.

[20] O. Christiansen, H. Koch, P. Jorgensen, The 2nd-order approximate coupled-cluster singles and doubles model CC2, Chem. Phys. Lett. 243 (1995) 409.

[21] C. Hättig, A. Köhn, Transition moments and excited-state first-order properties in the coupled-cluster model CC2 using the resolution-of-the-identity approximation, J. Chem. Phys. 117 (2002) 6939.

[22] C. Hättig, Geometry optimizations with the coupled-cluster model CC2 using the resolution-of-the-identity approximation, J. Chem. Phys. 118 (2003) 7751.

[23] A. Köhn, C. Hättig, Analytic gradients for excited states in the coupled-cluster model CC2 employing the resolution-of-the-identity approximation, J. Chem. Phys. 119 (2003) 5021.

[24] C. Hättig, Structure optimizations for excited states with correlated second-order methods: CC2 and ADC (2), Adv. Quant. Chem. 50 (2005) 37.

[25] F. Weigend, M. Häser, RI-MP2: first derivatives and global consistency, Theor. Chem. Acc. 97 (1997) 331.

[26] F. Weigend, R. Ahlrichs, Balanced basis sets of split-valence, triple-zeta valence and quadruple-zeta valence quality for H to Rn: Design an assessment of accuracy, Phys. Chem. Chem. Phys. 7 (2005) 3297.

[27] D. Andrae, U. Häußermann, M. Dolg, H. Stoll, H. Preuß, Energy-adjusted ab initio pseudopotentials for the second row and third row transition elements, Theor. Chim. Acta 77 (1990) 123.

[28] A. Klamt, G. Schüürmann, COSMO: a new approach to dielectric screening in solvents with explicit expressions for the screening energy and its gradient, J. Chem. Soc., Perkin Trans. 2 2 (1993) 799.

[29] M. J. Frisch, G. W. Trucks, H. B. Schlegel, G. E. Scuseria, M. A. Robb, J. R. Cheesem, G. Scalmani, V. Barone, B. Mennucci, G. A. Petersson, H. Nakatsuji, M. Caricato, X. Li, H. P. Hratchian, A. F. Izmaylov, J. Bloino, G. Zheng, J. L. Sonnenberg, M. Hada, M. Ehara, K. Toyota, R. Fukuda, J. Hasegawa, M. Ishida, T. Nakajima, Y. Honda, O. Kitao, H. Nakai, T. Vreven, J. A. M. Jr., J. E. Peralta, F. Ogliaro, M. Bearpark, J. J. Heyd, E. Brothers, K. N. Kudin, V. N. Staroverov, R. Kobayashi, J. Normand, K. Raghavachari, A. Rendell, J. C. Burant, S. S. Iyengar, J. Tomasi, M. Cossi, N. Rega, J. M. Millam, M. Klene, J. E. Knox, J. B. Cross, V. Bakken, C. Adamo, J. Jaramillo, R. Gomperts, R. E. Stratmann, O. Yazyev, A. J. Austin, R. Cammi, C. Pomelli, J. W. Ochterski, R. L. Martin, K. Morokuma, V. G. Zakrzewski, G. A. Voth, P. Salvador, J. J. Dannenberg, S. Dapprich, A. D. Daniels, O. Farkas, J. B. Foresman, J. V. Ortiz, J. Cioslowski, D. J. Fox, Gaussian 09, Revision B.01, Gaussian, Inc., Wallingford CT, 2010 (2010).

[30] G. Karlström, R. Lindh, P. Malmqvist, B. Roos, U. Ryde, V. Veryazov, P. Widmark, M. Cossi, B. Schimmelpfennig, P. Neogrady, L. Seijo, MOLCAS: a program package for computational chemistry, Comput. Mater. Sci. 28 (2003) 222.

[31] F. Aquilante, L. De Vico, N. Ferré, G. Ghigo, P. Malmqvist, P. Neogrády, T. Pedersen, M. Pitoňák, M. Reiher, B. Roos, L. Serrano-Andrès, M. Urban, V. Veryazov, R. Lindh, MOLCAS 7: the next generation, J. Comput. Chem. 31 (2010) 224.

[32] TURBOMOLE V6.3 2011, a development of University of Karlsruhe and Forschungszentrum Karlsruhe GmbH, 1989-2007, TURBOMOLE GmbH, since 2007; available from `http://www.turbomole.com`.

[33] H. Schmidbaur, A. Schier, A briefing on aurophilicity, Chem. Soc. Rev. 37 (2008) 1931.

[34] K. Peterson, C. Puzzarini, Systematically convergent basis sets for transition metals. II. Pseudopotential-based correlation consistent basis sets for the group 11 (Cu, Ag, Au) and 12 (Zn, Cd, Hg) elements, Theor. Chem. Acc. 114 (2005) 283.

[35] D. Figgen, G. Rauhut, M. Dolg, H. Stoll, Energy-consistent pseudopotentials for group 11 and 12 atoms: adjustment to multi-configuration Dirac–Hartree–Fock data, Chem. Phys. 311 (2005) 227.

[36] F. Weigend, M. Häser, H. Patzelt, R. Ahlrichs, RI-MP2: optimized auxiliary basis sets and demonstration of efficiency, Chem. Phys. Lett. 294 (1998) 143.

[37] B. Stevens, E. Hutton, Radiative life-time of the pyrene dimer and the possible role of excited dimers in energy transfer processes, Nature 186 (1960) 1045.

[38] J. Birks, Excimers and exciplexes, Nature 214 (1967) 1187.

[39] J. Birks, Excimers, Rep. Prog. Phys. 38 (1975) 903.

[40] M. Pabst, B. Lunkenheimer, A. Köhn, The triplet excimer of naphthalene a model system for triplet triplet interactions and its spectral properties, J. Phys. Chem. C 115 (2011) 8335.

[41] F. Plasser, H. Lischka, Analysis of excitonic and charge transfer interactions from quantum chemical calculations, J. Chem. Theory Comput. 8 (2012) 2777.

7. Cartesian Coordinates for All Optimized Structures

Default options for optimizations: Basis set, Au: LAN2TZf, C and N: 6-31G*; PCM model; MP2/PCM for S_0 state, CAM-B3LYP for T_1 state, and TD-CAM-B3LYP/PCM for S_1 state. If different options are employed, they are specified in parentheses.

1. Staggered S_0 dimer

			x(Å)	y(Å)	z(Å)
1	79	0	-1.507207	0.000240	-0.002778
2	6	0	-1.570804	1.401263	1.358507
3	6	0	-1.557349	-1.400683	-1.364912
4	7	0	-1.612498	2.253552	2.186015
5	7	0	-1.591796	-2.252810	-2.192924
6	79	0	1.506921	-0.000288	0.002757
7	6	0	1.556561	-1.400345	1.365805
8	6	0	1.572192	1.399850	-1.359367
9	7	0	1.615952	2.251968	-2.186943
10	7	0	1.591054	-2.252235	2.194060

2. Staggered T_1 dimer

1	79	0	1.348799	-0.000452	0.000344
2	6	0	1.496078	-1.339544	1.466187
3	6	0	1.499584	1.338558	-1.465269
4	7	0	1.508514	-2.126661	2.328116
5	7	0	1.514414	2.125768	-2.327074
6	79	0	-1.348759	0.000448	-0.000380
7	6	0	-1.497676	1.466213	1.338665
8	6	0	-1.498148	-1.465301	-1.339390
9	7	0	-1.512014	-2.327132	-2.126586
10	7	0	-1.511231	2.328126	2.125779

3. Eclipsed T_1 dimer

1	79	0	1.353923	0.004959	-0.000388
2	6	0	1.486775	1.907260	0.562853
3	6	0	1.505735	-1.896890	-0.560297
4	7	0	1.680050	2.999950	0.918788
5	7	0	1.711270	-2.987734	-0.914700
6	79	0	-1.353916	-0.005137	-0.000990
7	6	0	-1.503501	1.897152	-0.559981
8	6	0	-1.489018	-1.907012	0.563162
9	7	0	-1.683841	-2.999172	0.920027

10	7	0	-1.707548	2.988531	-0.9134730

4. Staggered S_1 dimer

1	79	0	1.355457	-0.108616	-0.001803
2	6	0	1.673599	1.283156	1.389532
3	6	0	1.197340	-1.515422	-1.399110
4	7	0	1.797642	2.101757	2.211169
5	7	0	1.021123	-2.335293	-2.210304
6	79	0	-1.355688	0.108641	0.001827
7	6	0	-1.202706	1.528468	-1.382881
8	6	0	-1.667270	-1.296520	1.380881
9	7	0	-1.787235	-2.122874	2.195333
10	7	0	-1.029757	2.356408	-2.186547

5. Eclipsed S_1 dimer

1	79	0	-1.366825	-0.002487	-0.000419
2	6	0	-1.527316	1.914398	-0.512393
3	6	0	-1.520134	-1.919698	0.512920
4	7	0	-1.738290	3.013184	-0.837578
5	7	0	-1.726278	-3.018701	0.840520
6	79	0	1.366821	0.002437	-0.000235
7	6	0	1.519133	1.919793	0.513084
8	6	0	1.528323	-1.914296	-0.512232
9	7	0	1.740051	-3.012975	-0.837423
10	7	0	1.724555	3.018888	0.840678

6. Staggered bent S_0 trimer

1	79	0	2.663383	0.455759	-0.091463
2	6	0	3.516021	-1.152086	0.625348
3	6	0	1.945072	2.118907	-0.821546
4	7	0	4.033324	-2.129983	1.061233
5	7	0	1.525935	3.134139	-1.276728
6	79	0	-0.000384	-0.917153	0.003205
7	6	0	-0.028952	-0.956894	1.957782
8	6	0	0.027296	-0.979937	-1.950575
9	79	0	-2.663344	0.459905	0.088120
10	6	0	-3.532831	-1.141611	-0.621940
11	6	0	-1.925916	2.117664	0.811308
12	7	0	0.045888	-1.023218	-3.138989
13	7	0	-0.046328	-0.983268	3.146709
14	7	0	-4.059603	-2.115903	-1.054554
15	7	0	-1.495925	3.129858	1.263553

7. Staggered linear S_0 trimer

1	79	0	-2.985967	0.002629	-0.000126
2	6	0	-3.048945	1.956290	-0.035871
3	6	0	-3.067911	-1.950139	0.035320
4	7	0	-3.081808	3.144586	-0.058656
5	7	0	-3.113512	-3.138014	0.057878
6	79	0	0.000178	-0.000458	0.000146
7	6	0	-0.000126	0.087700	1.953306
8	6	0	0.000526	-0.088698	-1.953012
9	79	0	2.986075	-0.002200	-0.000005
10	6	0	3.064972	1.950473	-0.049717
11	6	0	3.050809	-1.955563	0.049911
12	7	0	0.000717	-0.138698	-3.141092
13	7	0	-0.000402	0.137793	3.141383
14	7	0	3.108019	3.138239	-0.081285
15	7	0	3.084330	-3.143635	0.081657

8. Staggered linear T_1 trimer

1	79	0	-2.760891	0.005209	0.000006
2	6	0	-2.877221	1.991898	0.099197
3	6	0	-2.912873	-1.979336	-0.099134
4	7	0	-2.893041	3.156362	0.156927
5	7	0	-2.951825	-3.143243	-0.157114
6	79	0	0.000078	-0.000358	0.000080
7	6	0	-0.001463	-0.173244	1.978851
8	6	0	0.000994	0.172650	-1.978682
9	79	0	2.761411	-0.004972	-0.000082
10	6	0	2.909764	1.980928	0.074619
11	6	0	2.880201	-1.992593	-0.074997
12	7	0	0.001471	0.277000	-3.140415
13	7	0	-0.002538	-0.276909	3.140645
14	7	0	2.944182	3.145581	0.118174
15	7	0	2.895509	-3.157689	-0.118124

9. Staggered linear S_1 trimer

1	79	0	2.783292	0.007725	0.000046
2	6	0	2.867537	1.998357	-0.026633
3	6	0	2.919564	-1.980448	0.025219
4	7	0	2.868486	3.163917	-0.042646
5	7	0	2.952059	-3.145599	0.040059
6	79	0	-0.000425	-0.003346	0.000508
7	6	0	0.000995	-0.185159	-1.982233
8	6	0	-0.002196	0.177460	1.983352
9	79	0	-2.783478	-0.004416	-0.000310
10	6	0	-2.904659	1.978826	-0.156920
11	6	0	-2.878802	-1.988476	0.156472

12	7	0	-0.003481	0.286404	3.144097
13	7	0	0.001792	-0.294877	-3.142905
14	7	0	-2.928248	3.140657	-0.248537
15	7	0	-2.885807	-3.150563	0.247813

10. Staggered linear S_0 tetramer

1	79	0	4.450533	0.024129	-0.002970
2	6	0	4.491796	1.400099	-1.391704
3	6	0	4.572237	-1.344005	1.388217
4	7	0	4.514319	2.237404	-2.235883
5	7	0	4.648168	-2.176604	2.233868
6	79	0	1.475873	-0.026537	-0.000252
7	6	0	1.508837	-1.454395	-1.335606
8	6	0	1.481763	1.399127	1.338942
9	79	0	-1.475818	-0.013636	-0.000525
10	6	0	-1.491809	1.309314	-1.440633
11	6	0	-1.499571	-1.339670	1.436813
12	7	0	1.479411	2.265956	2.153442
13	7	0	1.524638	-2.323758	-2.147224
14	7	0	-1.497610	2.113740	-2.316791
15	7	0	-1.508699	-2.145329	2.311803
16	79	0	-4.450908	0.015149	0.003417
17	6	0	-4.544051	-1.406210	-1.336094
18	7	0	-4.599090	-2.270389	-2.151137
19	6	0	-4.518599	1.439496	1.341100
20	7	0	-4.558047	2.305870	2.154753

11. Staggered linear T_1 tetramer

1	79	0	4.249819	-0.028768	0.004817
2	6	0	4.327377	-1.352136	1.495012
3	6	0	4.442682	1.289632	-1.477695
4	7	0	4.346373	-2.126346	2.365523
5	7	0	4.536327	2.062811	-2.344165
6	79	0	1.362065	0.027731	-0.001282
7	6	0	1.416897	1.571790	1.252667
8	6	0	1.376087	-1.509058	-1.263046
9	79	0	-1.360721	0.015457	-0.000101
10	6	0	-1.397192	-1.224471	1.555028
11	6	0	-1.395932	1.251966	-1.557305
12	7	0	1.362301	-2.408959	-2.004360
13	7	0	1.427896	2.479332	1.984706
14	7	0	-1.399980	-1.950895	2.467079
15	7	0	-1.394223	1.975492	-2.471659
16	79	0	-4.252477	-0.013629	-0.003326
17	6	0	-4.392461	1.499353	1.286826
18	7	0	-4.446986	2.384364	2.042639
19	6	0	-4.375294	-1.532094	-1.289783

20	7	0	-4.418723	-2.420420	-2.042450

12. Staggered linear S_1 tetramer

1	79	0	4.278881	-0.046258	-0.010095
2	6	0	4.255873	-1.517914	1.334435
3	6	0	4.531167	1.413011	-1.345958
4	7	0	4.203038	-2.380225	2.116325
5	7	0	4.651516	2.268182	-2.128054
6	79	0	1.380129	0.035390	0.011444
7	6	0	1.440244	1.518404	1.342127
8	6	0	1.369955	-1.442702	-1.324303
9	79	0	-1.390136	-0.005240	0.004509
10	6	0	-1.431437	-1.330790	1.492765
11	6	0	-1.381532	1.316865	-1.485704
12	7	0	1.336503	-2.313445	-2.099039
13	7	0	1.461323	2.388072	2.117823
14	7	0	-1.442894	-2.100223	2.368237
15	7	0	-1.351625	2.090886	-2.356618
16	79	0	-4.271533	0.015855	-0.007425
17	6	0	-4.252148	1.504304	1.318308
18	7	0	-4.194541	2.372663	2.093510
19	6	0	-4.522686	-1.460236	-1.326035
20	7	0	-4.641394	-2.323866	-2.099336

13. Staggered linear S_0 pentamer

1	79	0	2.962900	-0.086403	0.007075
2	6	0	2.976524	0.006803	-1.946261
3	6	0	3.006514	-0.192395	1.959094
4	7	0	2.984564	0.062871	-3.134456
5	7	0	3.033170	-0.257020	3.146582
6	79	0	-0.000165	-0.115680	0.015039
7	6	0	-0.002002	-2.064036	-0.155715
8	6	0	0.000980	1.832447	0.187863
9	79	0	-2.962531	-0.085086	-0.004789
10	6	0	-2.980445	-0.017309	-1.958900
11	6	0	-3.000997	-0.165424	1.948848
12	7	0	0.001682	3.017459	0.292888
13	7	0	-0.003324	-3.249148	-0.259164
14	7	0	-2.990906	0.023497	-3.147676
15	7	0	-3.024186	-0.214548	3.137153
16	79	0	-5.939648	0.143233	-0.005399
17	6	0	-6.193616	-1.795318	0.001679
18	7	0	-6.346488	-2.974667	0.005827
19	6	0	-5.853071	2.096888	-0.013217
20	7	0	-5.797701	3.284821	-0.018208
21	79	0	5.939316	0.143388	-0.011619
22	6	0	5.855462	2.096946	0.002463

23	6	0	6.190945	-1.795337	-0.027068
24	7	0	5.802133	3.284949	0.011104
25	7	0	6.342250	-2.974834	-0.036478

14. Staggered linear T_1 pentamer

1	79	0	2.762679	-0.063401	0.005848
2	6	0	2.808550	0.007672	-1.984440
3	6	0	2.833663	-0.141392	1.995315
4	7	0	2.805836	0.046530	-3.149507
5	7	0	2.846817	-0.187940	3.159957
6	79	0	-0.000792	-0.077923	0.008978
7	6	0	-0.005644	-2.062952	-0.108582
8	6	0	0.003030	1.907132	0.129577
9	79	0	-2.765136	-0.060235	-0.003269
10	6	0	-2.811754	-0.006007	-1.994643
11	6	0	-2.832931	-0.117879	1.987189
12	7	0	0.006878	3.070731	0.201109
13	7	0	-0.008484	-3.226917	-0.176659
14	7	0	-2.810365	0.023592	-3.159847
15	7	0	-2.844710	-0.152384	3.152226
16	79	0	-5.825265	0.099819	-0.003689
17	6	0	-6.060168	-1.879901	0.012915
18	7	0	-6.181777	-3.038073	0.022811
19	6	0	-5.799311	2.093459	-0.020621
20	7	0	-5.767373	3.257521	-0.032412
21	79	0	5.827756	0.099732	-0.006967
22	6	0	5.810049	2.093078	0.021111
23	6	0	6.055339	-1.880430	-0.040728
24	7	0	5.785793	3.257363	0.035459
25	7	0	6.175230	-3.038722	-0.060817

15. Staggered linear S_1 pentamer

1	79	0	2.813326	0.009421	-0.000174
2	6	0	2.852503	-0.140778	1.987839
3	6	0	2.844124	0.160890	-1.988403
4	7	0	2.851860	-0.232297	3.149638
5	7	0	2.838065	0.250926	-3.150325
6	79	0	0.008150	-0.008936	0.010262
7	6	0	-0.000548	1.984320	0.010010
8	6	0	0.012125	-2.002244	0.011594
9	79	0	-2.802156	-0.014324	0.004711
10	6	0	-2.850129	0.144085	1.992058
11	6	0	-2.834453	-0.173186	-1.982838
12	7	0	0.013779	-3.167599	0.012601
13	7	0	-0.004568	3.149672	0.010620
14	7	0	-2.855429	0.239393	3.153471
15	7	0	-2.829862	-0.268009	-3.144334

16	79	0	-5.824532	0.015201	-0.008237
17	6	0	-5.914154	1.997530	-0.208815
18	7	0	-5.946545	3.155270	-0.332057
19	6	0	-5.967208	-1.964270	0.189385
20	7	0	-6.032478	-3.121282	0.306870
21	79	0	5.806810	-0.001427	-0.005666
22	6	0	5.907314	-1.984133	-0.200526
23	6	0	5.945084	1.978780	0.187521
24	7	0	5.945102	-3.142707	-0.315292
25	7	0	6.006630	3.136511	0.300555

16. Staggered S_0 dimer (RI-CC2/def2-TZVP in vacuo)

Au	1.5248992	0.1350898	-0.0216413
C	1.8100376	-1.3185246	-1.3105531
C	1.5228391	1.6148619	1.2694453
N	2.0814343	-2.1779611	-2.0801546
N	1.6236799	2.5075394	2.0424466
Au	-1.5175480	-0.1344074	-0.0076776
C	-1.5166236	-1.4438652	1.4557031
C	-1.7981870	1.1503562	-1.4660200
N	-2.0660996	1.9092730	-2.3360440
N	-1.6151099	-2.2340679	2.3334315

17. Staggered T_1 dimer (RI-CC2/def2-TZVP in vacuo)

Au	1.2922364	0.1120603	-0.0154753
C	1.4734148	-1.3485081	-1.3096141
C	1.1822533	1.5823567	1.2740102
N	1.5841576	-2.2315124	-2.0953957
N	1.1095013	2.4744097	2.0538114
Au	-1.2822619	-0.1090434	-0.0023976
C	-1.1775245	-1.4104807	1.4577537
C	-1.4582505	1.1808501	-1.4672850
N	-1.5643773	1.9595978	-2.3569606
N	-1.1098271	-2.2014361	2.3404889

18. Staggered S_1 dimer (RI-CC2/def2-TZVP in vacuo)

Au	1.3060404	0.0745587	-0.0071387
C	1.5295595	-1.3854861	-1.3057163
C	1.1946257	1.5519785	1.2785625
N	1.6344586	-2.2637967	-2.0985159
N	1.0856712	2.4489350	2.0500500
Au	-1.2972371	-0.0712965	0.0009728
C	-1.1862702	-1.3797570	1.4583339
C	-1.5159404	1.2176052	-1.4682454
N	-1.6200654	1.9911048	-2.3635476
N	-1.0815202	-2.1755519	2.3341807

19. Staggered S_0 dimer (MP2 in vacuo)

1	79	0	1.586178	-0.000057	-0.000829
2	6	0	1.711050	-1.385363	1.383640
3	6	0	1.706502	1.385275	-1.385698
4	7	0	1.882443	-2.218969	2.216431
5	7	0	1.875230	2.218879	-2.219034
6	79	0	-1.586178	0.000041	0.000828
7	6	0	-1.706217	1.384955	1.386142
8	6	0	-1.711335	-1.384802	-1.384077
9	7	0	-1.882904	-2.218103	-2.217137
10	7	0	-1.874778	2.218319	2.219752

20. Staggered T_1 dimer (CAM-B3LYP in vacuo)

1	79	0	-1.355279	-0.000168	0.000257
2	6	0	-1.509837	-1.360539	1.454414
3	6	0	-1.511848	1.360073	-1.453841
4	7	0	-1.591421	-2.155990	2.304705
5	7	0	-1.594709	2.155456	-2.304071
6	79	0	1.355456	0.000174	-0.000249
7	6	0	1.510346	-1.454072	-1.360447
8	6	0	1.510630	1.454489	1.359848
9	7	0	1.592596	2.304904	2.155130
10	7	0	1.592141	-2.304399	-2.155840

21. Staggered S_0 dimer (MP2/PCM, cc-pVDZ for C and N, cc-pVDZ-PP for Au)

1	79	0	-1.504181	-0.000477	-0.019347
2	6	0	-1.604380	1.392777	1.361582
3	6	0	-1.506187	-1.394064	-1.404488
4	7	0	-1.667184	2.237879	2.199731
5	7	0	-1.508087	-2.238931	-2.245244
6	79	0	1.503820	0.000392	0.019220
7	6	0	1.508132	-1.395037	1.402566
8	6	0	1.602768	1.395987	-1.359440
9	7	0	1.664744	2.242432	-2.196297
10	7	0	1.514318	-2.240137	2.243062

22. Staggered S_0 dimer (MP2 in vacuo, cc-pVDZ for C and N, cc-pVDZ-PP for Au)

1	79	0	1.576377	0.003832	0.000039
2	6	0	1.707171	-1.388788	-1.390558
3	6	0	1.684861	1.398240	1.390875
4	7	0	1.874784	-2.224942	-2.226460
5	7	0	1.839323	2.236814	2.226885
6	79	0	-1.576374	-0.003837	-0.000103
7	6	0	-1.685244	-1.399021	1.389930

8	6	0	-1.706793	1.389574	-1.389949
9	7	0	-1.874179	2.226185	-2.225438
10	7	0	-1.839959	-2.238002	2.225481

23. Staggered S_0 dimer (MP2/PCM, cc-pVTZ for C and N, cc-pVDZ-PP for Au)

1	79	0	-1.475368	0.000081	-0.011156
2	6	0	-1.550374	1.416253	1.345444
3	6	0	-1.495436	-1.415561	-1.370733
4	7	0	-1.589963	2.278068	2.168756
5	7	0	-1.501772	-2.275857	-2.196568
6	79	0	1.475311	-0.000456	0.011098
7	6	0	1.494428	-1.415863	1.370944
8	6	0	1.551191	1.415643	-1.345520
9	7	0	1.592316	2.277320	-2.168895
10	7	0	1.500221	-2.275710	2.197253

24. Staggered S_0 dimer (MP2 in vacuo, cc-pVTZ for C and N, cc-pVDZ-PP for Au)

1	79	0	-1.557416	-0.000044	0.002165
2	6	0	-1.672308	-1.388550	-1.391720
3	6	0	-1.660389	1.388550	1.396959
4	7	0	-1.827953	-2.224878	-2.230717
5	7	0	-1.808883	2.224930	2.237198
6	79	0	1.557428	0.000011	-0.002164
7	6	0	1.660253	1.394818	-1.390758
8	6	0	1.672422	-1.394695	1.385508
9	7	0	1.828098	-2.234746	2.220770
10	7	0	1.808624	2.234965	-2.227252

25. Staggered S_0 dimer (MP2/PCM, def2-TZVP for C and N, def2-TZVPPD for Au)

1	79	0	-1.488189	0.006105	-0.000143
2	6	0	-1.547194	-1.405595	1.348955
3	6	0	-1.516262	1.419468	-1.348943
4	7	0	-1.583400	-2.257214	2.161047
5	7	0	-1.535669	2.272128	-2.160533
6	79	0	1.488752	-0.006182	0.000073
7	6	0	1.516392	-1.420510	-1.347796
8	6	0	1.546125	1.406764	1.347993
9	7	0	1.580230	2.259289	2.159225
10	7	0	1.533294	-2.273441	-2.159129

26. Staggered S_0 dimer (MP2 in vacuo, def2-TZVP for C and N, def2-TZVPPD for Au)

1	79	0	1.574623	0.000231	-0.000654
2	6	0	1.688455	-1.752164	0.875566
3	6	0	1.684334	1.752746	-0.877222
4	7	0	1.842441	-2.798015	1.398434

5	7	0	1.835962	2.798692	-1.400588
6	79	0	-1.574585	-0.000216	0.000653
7	6	0	-1.684381	0.876192	1.753248
8	6	0	-1.688401	-0.876750	-1.751588
9	7	0	-1.842588	-1.399924	-2.797257
10	7	0	-1.836247	1.399055	2.799411

27. Staggered S_0 dimer (MP2/PCM, 6-31G* for C and N, LANL2DZ for Au)

1	79	0	1.601443	-0.028346	0.000189
2	6	0	1.709735	1.468226	1.330705
3	6	0	1.572990	-1.529789	-1.329415
4	7	0	1.773835	2.353030	2.120502
5	7	0	1.555951	-2.420339	-2.115184
6	79	0	-1.601406	0.028116	-0.001178
7	6	0	-1.570475	1.529591	-1.330743
8	6	0	-1.712701	-1.467104	1.330651
9	7	0	-1.778833	-2.351754	2.120453
10	7	0	-1.550983	2.420866	-2.115639

28. Staggered T_1 dimer (CAM-B3LYP/PCM, cc-pVDZ for C and N, cc-pVDZ-PP for Au)

1	79	0	1.352014	-0.013218	0.014250
2	6	0	1.567170	1.267340	-1.510009
3	6	0	1.444124	-1.295687	1.547107
4	7	0	1.624129	2.022792	-2.399594
5	7	0	1.419372	-2.039697	2.447958
6	79	0	-1.351885	0.012342	-0.015578
7	6	0	-1.504165	-1.519308	-1.295063
8	6	0	-1.507141	1.544328	1.263024
9	7	0	-1.526070	2.442635	2.010118
10	7	0	-1.518881	-2.412994	-2.047831

29. Staggered T_1 dimer (CAM-B3LYP in vacuo, cc-pVDZ for C and N, cc-pVDZ-PP for Au)

1	79	0	1.359609	-0.001208	0.002559
2	6	0	1.529186	1.416075	1.415876
3	6	0	1.535508	-1.418621	-1.409970
4	7	0	1.620645	2.240552	2.238916
5	7	0	1.631025	-2.243812	-2.231823
6	79	0	-1.359638	0.001013	-0.002684
7	6	0	-1.523431	1.416749	-1.418115
8	6	0	-1.541175	-1.413646	1.411995
9	7	0	-1.640079	-2.236313	2.235975
10	7	0	-1.611345	2.241300	-2.241475

30. Staggered T_1 dimer (CAM-B3LYP/PCM, cc-pVTZ for C and N, cc-pVDZ-PP for Au)

1	79	0	1.342181	0.096042	-0.008991

2	6	0	1.691456	-1.368697	-1.325813
3	6	0	1.273484	1.580878	1.323145
4	7	0	1.825144	-2.230037	-2.103989
5	7	0	1.144464	2.446923	2.097207
6	79	0	-1.342549	-0.096247	0.005300
7	6	0	-1.264797	-1.425864	1.491788
8	6	0	-1.699390	1.214046	-1.463326
9	7	0	-1.836945	1.984575	-2.330910
10	7	0	-1.129164	-2.199459	2.357239

31. Staggered T_1 dimer (CAM-B3LYP in vacuo, cc-pVTZ for C and N, cc-pVDZ-PP for Au)

1	79	0	-1.352053	-0.033538	0.008456
2	6	0	-1.598050	1.154977	-1.588715
3	6	0	-1.419749	-1.238038	1.609011
4	7	0	-1.737287	1.843752	-2.521905
5	7	0	-1.446131	-1.944743	2.539074
6	79	0	1.352207	0.034516	-0.008684
7	6	0	1.433997	1.639368	1.189624
8	6	0	1.583361	-1.558753	-1.204896
9	7	0	1.713153	-2.485205	-1.904549
10	7	0	1.468899	2.577252	1.885646

32. Staggered T_1 dimer (CAM-B3LYP/PCM, def2-TZVP for C and N, def2-TZVPPD for Au)

1	79	0	-1.349475	-0.003045	0.021671
2	6	0	-1.556440	-1.244925	-1.533940
3	6	0	-1.460210	1.244877	1.581042
4	7	0	-1.607124	-1.964139	-2.439587
5	7	0	-1.447734	1.965144	2.487149
6	79	0	1.349468	0.001378	-0.021828
7	6	0	1.461365	1.564495	-1.264969
8	6	0	1.555291	-1.555338	1.218871
9	7	0	1.605270	-2.457972	1.941900
10	7	0	1.449671	2.467968	-1.988554

33. Staggered T_1 dimer (CAM-B3LYP in vacuo, def2-TZVP for C and N, def2-TZVPPD for Au)

1	79	0	1.357464	0.000051	0.000215
2	6	0	1.537927	1.419192	1.408381
3	6	0	1.538998	-1.418607	-1.408394
4	7	0	1.637690	2.237479	2.220441
5	7	0	1.639571	-2.236724	-2.220661
6	79	0	-1.357473	-0.000185	-0.000226
7	6	0	-1.538428	1.408816	-1.418473
8	6	0	-1.538489	-1.408811	1.418491
9	7	0	-1.638634	-2.221132	2.236558
10	7	0	-1.638528	2.221381	-2.236211

34. Staggered S_1 dimer (in vacuo, RI-ADC(2)/def2-TZVP)

Au	1.3127337	0.0748918	-0.0069113
C	1.5289457	-1.3850059	-1.3052605
C	1.1945903	1.5511183	1.2779583
N	1.6335742	-2.2563482	-2.0918243
N	1.0858460	2.4410862	2.0432815
Au	-1.3029705	-0.0716046	0.0010212
C	-1.1873346	-1.3789586	1.4577353
C	-1.5159699	1.2170855	-1.4674530
N	-1.6189350	1.9846310	-2.3561391
N	-1.0811579	-2.1686014	2.3265279

35. Staggered T_1 dimer (in vacuo, RI-ADC(2)/def2-TZVP)

Au	1.2997577	0.1133958	-0.0159336
C	1.4748238	-1.3469717	-1.3086982
C	1.1837176	1.5813649	1.2729409
N	1.5818031	-2.2237789	-2.0881975
N	1.1093818	2.4663135	2.0471973
Au	-1.2896965	-0.1105099	-0.0028478
C	-1.1793673	-1.4097151	1.4564846
C	-1.4594040	1.1793332	-1.4661495
N	-1.5622771	1.9529531	-2.3488791
N	-1.1094170	-2.1940909	2.3330189

36. Staggered S_0 dimer (in vacuo, RI-MP2/def2-TZVP)

Au	1.5858920	0.1409290	-0.0208810
C	1.8390340	-1.3137150	-1.3099760
C	1.5546740	1.6164470	1.2690430
N	2.0651320	-2.1755050	-2.0787430
N	1.6092220	2.5044750	2.0394480
Au	-1.5765990	-0.1396260	-0.0060840
C	-1.5467720	-1.4450200	1.4557980
C	-1.8275700	1.1453000	-1.4648430
N	-2.0507420	1.9065330	-2.3340380
N	-1.6029490	-2.2315230	2.3292120

37. Staggered S_0 dimer (in vacuo, RI-CC2/def2-SVP)

Au	1.5743625	0.1384385	-0.0210706
C	1.8326334	-1.3395296	-1.3305124
C	1.5406246	1.6377685	1.2896273
N	2.0775212	-2.2102110	-2.1087867
N	1.6112462	2.5377254	2.0699282
Au	-1.5654203	-0.1373569	-0.0066784
C	-1.5337348	-1.4638567	1.4786345
C	-1.8204681	1.1685748	-1.4882541

N	-2.0630718	1.9373160	-2.3680101
N	-1.6043708	-2.2605752	2.3640583

38. Staggered T_1 dimer (in vacuo, RI-CC2/def2-SVP)

Au	1.3190271	0.1089900	-0.0126699
C	1.4891955	-1.3729836	-1.3274145
C	1.1972459	1.6012494	1.2944548
N	1.5824296	-2.2611532	-2.1215508
N	1.1110679	2.5009646	2.0764429
Au	-1.3106576	-0.1062563	-0.0008377
C	-1.1896060	-1.4266753	1.4798338
C	-1.4769825	1.2024954	-1.4886422
N	-1.5681785	1.9855861	-2.3867743
N	-1.1042195	-2.2239231	2.3660940

39. Staggered S_1 dimer (in vacuo, RI-CC2/def2-SVP)

Au	1.3381660	0.0657937	-0.0000899
C	1.5574443	-1.4127917	-1.3205095
C	1.2091929	1.5658864	1.2989552
N	1.6389263	-2.2922331	-2.1271879
N	1.0707548	2.4723722	2.0673810
Au	-1.3281748	-0.0617439	0.0068665
C	-1.2026911	-1.3910620	1.4806697
C	-1.5445247	1.2429843	-1.4861187
N	-1.6238949	2.0157991	-2.3953874
N	-1.0658767	-2.1967109	2.3543570

40. Staggered S_0 dimer (in vacuo, RI-MP2/def2-SVP)

Au	1.6221602	0.1445072	-0.0206040
C	1.8524626	-1.3341990	-1.3289207
C	1.5636043	1.6392377	1.2881031
N	2.0612372	-2.2056961	-2.1052917
N	1.5998980	2.5332305	2.0653487
Au	-1.6127609	-0.1427747	-0.0057894
C	-1.5561414	-1.4653474	1.4773125
C	-1.8405511	1.1635212	-1.4861656
N	-2.0469432	1.9329245	-2.3639272
N	-1.5936438	-2.2571100	2.3588703